Imaging Mouse Retinal Ganglion Cells and Their Loss In Vivo by a Fundus Camera in the Normal and Ischemia-Reperfusion Model

Hiroshi Murata,[1] *Makoto Aihara,*[2] *Yi-Ning Chen,*[2] *Takashi Ota,*[2] *Jiro Numaga,*[1] *and Makoto Araie*[2]

Purpose. To visualize retinal ganglion cells (RGCs) and their gradual loss in the living mouse.

Methods. With the use of B6.Cg-Tg(Thy1-CFP)23Jrs/J mice, which express cyan fluorescent protein (CFP) in RGCs, and a commercially available mydriatic retinal camera attached with a 5 million-pixel digital camera to visualize RGCs in vivo, the authors recorded fundus photographs longitudinally in the ischemia reperfusion model group and the untreated group to evaluate longitudinal changes in the number of RGCs in experimental models. Moreover, RGCs expressing CFP were evaluated histologically by a retrograde-labeling method and retinal whole mount or sections.

Results. The authors devised an in vivo imaging technique using a conventional retinal camera and visualized RGCs at the single-cell level. In the ischemia reperfusion model, a longitudinal reduction in the number of RGCs was demonstrated in each mouse eye. The number of RGCs and the fluorescence intensity of the nerve fiber decreased considerably during the first week. The percentages of RGCs decreased to 34.2% ± 7.5%, 24.1% ± 9.1%, 23.0% ± 9.3%, and 22.2% ± 8.4% (mean ± SD, $n = 5$) of the percentages before injury at 1, 2, 3, and 4 weeks after injury, respectively ($P < 0.001$). In this transgenic mouse, 97% of CFP-expressing cells were RGCs and 73% of RGCs expressed CFP.

Conclusions. This in vivo technique allows noninvasive, repeated, and longitudinal evaluation of RGCs for investigation of retinal neurodegenerative diseases and new therapeutic modalities for them. (*Invest Ophthalmol Vis Sci.* 2008;49:5546–5552) DOI:10.1167/iovs.07-1211

The neural retina and the optic disc are the only neuronal tissues that can be visualized in vivo without any invasive manipulation, and a great improvement has recently been achieved in imaging techniques for the evaluation of the human retina and optic nerve head (ONH).[1,2] Glaucoma, the second leading cause of vision loss in the world,[3] is associated with damage of optic nerve axons at the ONH and their cell bodies, the retinal ganglion cells (RGCs).[4] The only therapy available to stem RGC death in glaucoma is the reduction of intraocular pressure (IOP),[5] which is especially effective in patients with elevated IOP. However, elevated IOP is not the only pathogenic factor of glaucoma.[6]

Experimental neurodegenerative models such as ischemia reperfusion, optic nerve crush, intravitreal glutamate injection, and experimental ocular hypertension[7] have been used to investigate the pathogenesis of RGC death and possible neuroprotective treatment against it, for which reliable evaluation of the number of living RGCs was indispensable. As an experimental animal, the mouse has great advantages not only because it is less expensive and more easily handled than other animals but also because of the availability of various knockout or transgenic mice, enabling investigation of the role of a molecule in vivo. Until now, however, a technique allowing in vivo, noninvasive, and longitudinal observation of RGCs in the living mouse has not been established.

In the present study, we report a method of noninvasive visualization and quantitation of RGCs using B6.Cg-Tg(Thy1-CFP)23Jrs/J[8] mice. The strain expresses cyan fluorescent protein (CFP; major excitation peak, 433 nm; major emission peak, 475 nm),[9] in RGCs under the control of neuron-specific elements from the *Thy1* gene.[8] We evaluated longitudinal changes in the number of RGCs in the living mouse that underwent retinal ischemia reperfusion.[7]

Materials and Methods

Retinal Camera System

We used a commercially available mydriatic retinal camera (TRC-50IX; Topcon, Tokyo, Japan) attached with a 5 million-pixel digital camera (Nikon D1x; Nikon, Tokyo, Japan). The settings of the retinal camera were as follows: pupil, normal; image angle, 50°; flash, 300. The settings of the digital camera were as follows: shutter speed, 1/30 second; ISO, 800; image quality, fine. A 40-diopter aspherical lens (40D; Volk Optical, Mentor, OH) was fixed in front of the objective lens of the retinal camera at a distance of 5 mm, and the optical axis was adjusted. Built-in filters for fluorescein angiography were used for the fluorescein angiogram, band-pass filters, D436/20x (center wavelength, 436 nm; full width at half maximum [FWHM] transmission, 20 nm; Chroma Technology, Rockingham, VT), and BI0049 (center wavelength, 494 nm; FWHM transmission, 33 nm; Asahi Spectra, Tokyo, Japan) were used for the detection of CFP fluorescence. All images were captured with software (IMAGEnet; Topcon) and were saved by 3008 × 1960 × 8 bit-tagged image file format (TIFF). To improve the signal-to-noise ratio, a series of three images was taken for each measurement. The images were aligned automatically (AutoDeblur; Media-Cybernetics, Silver Spring, MD) and were combined (MaxIm DL 4.0; Diffraction Limited, Ontario, BC, Canada).

Ocular Fundus Photography

Three microliters of ophthalmic solution containing 0.5% tropicamide and 0.5% phenylephrine hydrochloride (Mydrin-P; Santen Pharmaceu-

From the [1]Tokyo Metropolitan Geriatric Hospital, Tokyo, Japan; and the [2]Department of Ophthalmology, University of Tokyo School of Medicine, Tokyo, Japan.

Supported in part by Grant H18-Kankakuippan-001 from the Ministry of Health, Labor, and Welfare of Japan and by Grant A18209053 from the Ministry of Education, Culture, Sports, Science and Technology of Japan (MAr).

Submitted for publication September 16, 2007; revised January 6, March 6, and June 25, 2008; accepted October 21, 2008.

Disclosure: **H. Murata**, None; **M. Aihara**, None; **Y.-N. Chen**, None; **T. Ota**, None; **J. Numaga**, None; **M. Araie**, None

The publication costs of this article were defrayed in part by page charge payment. This article must therefore be marked "*advertisement*" in accordance with 18 U.S.C. §1734 solely to indicate this fact.

Corresponding author: Makoto Aihara, Department of Ophthalmology, University of Tokyo School of Medicine, 7-3-1 Hongo, Bunkyo-ku Tokyo 113-8655, Japan; aihara-tky@umin.ac.jp.

tical, Osaka, Japan) was applied topically 10 minutes before anesthesia to dilate the pupil, and then mice were anesthetized with intraperitoneal injection of a mixture of ketamine (100 mg/kg body weight) and xylazine (9 mg/kg body weight). To avoid corneal injury, mice were restrained manually until they were anesthetized. A few minutes later, the mice were confirmed by the disappearance of the ciliary reflex to be fully anesthetized, and the cornea was covered carefully with mineral oil (Johnson's Baby Oil; Johnson & Johnson, New Brunswick, NJ) to prevent desiccation and to keep the surface smooth. Smoothness of the corneal surface and transparency were confirmed under an operation microscope. The laterality of the recorded eyes was chosen randomly. All the images were taken by an experienced investigator (HM).

Fluorescein Angiography

A 12-week-old C57BL/6 mouse was used. Ten microliters of fluorescein sodium (10% Fluorescite; Alcon Japan, Tokyo, Japan) was injected into the tail vein, and angiograms were obtained after 5 minutes. Fundus images were obtained using the retinal camera system, as described.

Animal Husbandry

Adult male and female B6.Cg-Tg(Thy1-CFP)23Jrs/J mice[8] were obtained from the breeding colony of The Jackson Laboratory (Bar Harbor, ME). The environment was kept at 23°C with a 12-hour light/12-hour dark cycle. All mice were fed ad libitum. Ten- to 15-week-old mice weighing 20 to 30 g were used. All studies were in compliance with the ARVO Statement for the Use of Animals in Ophthalmic and Vision Research.

Retrograde Labeling of RGCs in the Untreated Group and the Ischemia Reperfusion Group

To investigate the distribution of CFP in the retina, retrograde labeling with 1,1′-dioctadecyl-3,3,3′,3′-tetramethylindocarbocyanine perchlorate (DiI) was performed. Three B6.Cg-Tg (Thy1-CFP)23Jrs/J[8] mice were anesthetized and placed in a stereotactic frame. The skull was exposed and kept dry. Two holes were made at 2.92 mm behind the bregma in the anteroposterior axis and 0.5 mm lateral to the midline, and 5% DiI (1 μL at a rate of 0.5 μL/min; Molecular Probes, Eugene, OR) in dimethyl sulfoxide was injected at a depth of 2 mm from the brain surface into the superior colliculus of both sides. Ten days after injection, the mice were killed, and each eye was enucleated and fixed immediately in 4% paraformaldehyde in 0.1 M phosphate-buffered saline (PBS) for 30 minutes at 4°C. After the cornea and lens were removed, the sample was fixed again for 2 hours. Four radial relaxing incisions were made, the retina was prepared as a flattened whole mount on a glass slide with a coverslip, and an image was obtained with a fluorescence microscope (BX50; Olympus, Tokyo, Japan) with appropriate filters. Four square areas of 370 × 370 μm at a distance of approximately 1.5 mm from the optic nerve head were selected, and the number of cells was counted manually by an experienced investigator (MAi). Results were averaged for the four quadrant areas to obtain a value representing the eyes in question.

The same procedure was performed in the ischemia reperfusion group. Three weeks after ischemia reperfusion injury, DiI was injected into five mice of the ischemia reperfusion injury group. Seven days after injection, the retina was whole mounted. Then DiI^+ cells among CFP-expressing cells and CFP^+ cells among DiI^+ cells were counted and compared with those in untreated control eyes by an unpaired *t*-test. $P < 0.05$ was considered statistically significant.

Frozen Section

Localization of CFP^+ cells in the retina was assessed by retinal frozen sections. Four eyes of two thy1-CFP mice were enucleated, fixed in 4% paraformaldehyde in 0.1 M PBS for 1 hour, and fixed again for 1 hour after the removal of the cornea and lens. The globes were embedded (Tissue-Tek O.C.T.; Sakura Finetechnical, Tokyo, Japan) and cryopreserved in 15-mm-thick frozen sections, and sequential meridian sections (5-μm thick) were made through the optic disc. Sections were mounted on a glass slide with antifade medium containing propidium iodide (VectaShield with propidium iodide H-1300: Vector Laboratories, Burlingame, CA) to stain nuclei.

Comparison of a Mouse Fundus Photograph with a Whole Mount Retinal Image

Immediately after fundus photographs were obtained from a B6.Cg-Tg (Thy1-CFP) 23Jrs/J mouse,[8] the mouse was killed, and the retina was whole mounted and photographed with a fluorescence microscope (MZFLIII; Leica Microsystems Japan, Tokyo, Japan).

Ischemia Reperfusion Injury

Five mice were used for the ischemia reperfusion injury model.[10] Sodium pentobarbital (50 mg/kg body weight) was administered intraperitoneally. After anesthesia, the anterior chamber of the right eye was cannulated with a microneedle[11] connected to a reservoir filled with intraocular irrigating solution (BSS Plus; Santen Pharmaceutical). Retinal ischemia was induced by elevating the reservoir, and the IOP was raised to 110 mm Hg for 60 minutes.[12] During ischemia, the IOP was monitored continuously, the room temperature was maintained at 25°C,[13] and the room was kept dark. Ocular fundus images were recorded as described at five time points, just before injury and 1, 2, 3, and 4 weeks after it. Seven mice underwent sham operation by cannulation of the microneedle without elevation of the intracameral pressure and were used as controls. Their retinal images were recorded five times at 1-week intervals.

Reproducibility of Counting and Regional Difference of the Number of RGCs

We took fundus photographs of 10 eyes of five mice. Bilateral eyes of each mouse underwent fundus photography twice at intervals of 24 hours. The number of RGCs in the same area of the four square fields (220 × 220 pixels) was counted manually. Moreover, cell density was counted in each of four areas to investigate the regional differences of sampled area in each quadrant located 800 μm apart from the optic disc.

RGC Counting in Fundus Photographs and Retinal Flat Mount

Four square fields of 220 × 220 pixels (approximately 370 × 370 μm), one field from each quadrant of the retina, at a distance of approximately 800 μm from the optic nerve disc was always used for RGC counting in the fundus photograph or retinal flat mount, respectively. The number of cells emitting fluorescence was counted manually. Cell counting was performed by an experienced investigator (MAi) who was masked to the experimental treatment of the eye.

The numbers of RGCs counted in four square fields in the retina of ischemia reperfusion eyes were normalized to those obtained identically in the control eyes and were indicated as RGC survival rate. Each percentage is expressed in the text and figures as the mean ± SD. The difference in RGC density among four areas was statistically analyzed by a Kruskal-Wallis test. $P < 0.05$ was considered statistically significant.

Histologic Evaluation

After the last fundus photograph was taken at 4 weeks, one mouse was chosen randomly from the sham-operated control group and the ischemia reperfusion injury group. The mice were killed, and their eyes were enucleated, fixed in 4% paraformaldehyde and 2.5% glutaraldehyde in 0.1 M PBS for 1 hour, and fixed again for 24 hours after removal of the cornea and lens. The globes were processed to paraffin-embedded sections, and sequential meridian sections (5-μm thick) were made through the optic disc. Sections were stained with hematoxylin and eosin. Sections were examined with a light microscope (BX50; Olympus).

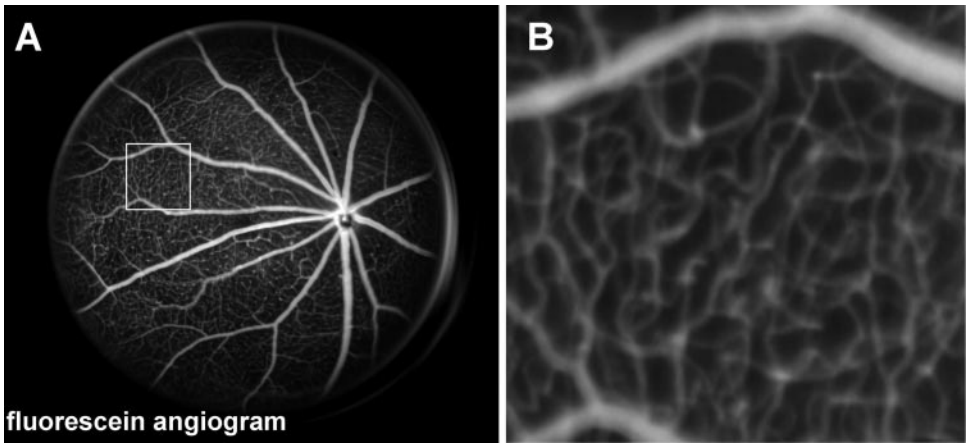

FIGURE 1. (**A**) Fluorescein angiogram of the mouse ocular fundus. (**B**) Area corresponding area to the *insert* in (**A**).

RESULTS

Mouse Fundus Photography

At first, to examine the resolving power of the fundus photograph with our method, we took a fundus fluorescein angiogram of a C57BL/6J mouse (Figs. 1A, 1B).

A wide area of retina was recorded, and blood capillaries were visualized with sufficient quality. Comparison of the fluorescein angiogram with those obtained from other studies suggested that the resolving power provided by our system was similar to that provided by a 10° view of a confocal scanning laser ophthalmoscope (cSLO) and superior to a 20° view of it,[14–16] whereas the area recorded by our system was similar to that provided by a 20° view of a cSLO.

Investigation of CFP Expression in the Mouse Retina

To identify the distribution of CFP in the B6.Cg-Tg(Thy1-CFP)23Jrs/J[8] mouse retina, retrograde labeling of RGCs with DiI was performed in five untreated eyes of three mice. Colo-

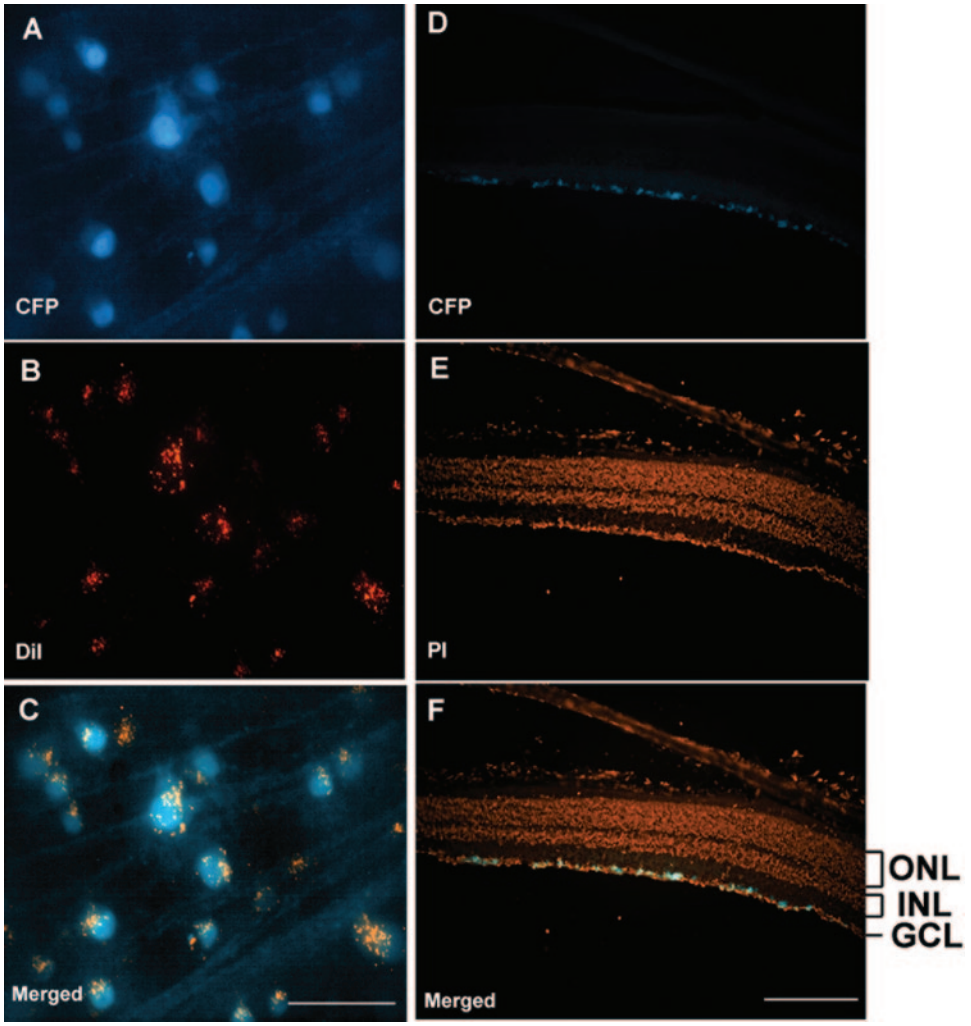

FIGURE 2. (**A–C**) Double labeling of RGCs with CFP and DiI. (**A**) RGCs expressing CFP. (**B**) Same field of DiI optics. (**C**) Merged image of (**A**) and (**B**). (**D–F**) Frozen section of Thy-1 CFP mouse. CFP was expressed only in the ganglion cell layer. Scale bars, (**A–C**) 50 μm; (**D–F**) 200 μm.

TABLE 1. Types of Labeling with CFP and DiI in Ischemia Reperfusion Group and Control Group

Cells	Control (%)	Ischemia Reperfusion (%)
DiI^+ among CFP^+	97.0	97.8
DiI^- among CFP^+	3.0	2.2
CFP^+ among DiI^+	72.6	59.2
CFP^- among DiI^+	27.4	40.8

calization of CFP and DiI in the same cells was observed (Figs. 2A–2C). Among the CFP^+ cells, DiI^+ cells accounted for 97.0% ± 2.7% (mean ± SD, $n = 5$) and DiI^- cells accounted for 3.0% ± 2.7%. Among the DiI^+ cells, CFP^+ cells accounted for 72.6% ± 5.2%, and CFP^- cells accounted for 27.4% ± 5.2% (Table 1). The density of DiI^+ cells was 2100 ± 136 cells/μm^2. Figures 2D–2F indicated that all the CFP^+ cells were localized only in the RGC layer.

Visualization of RGCs In Vivo and Comparison of a Fundus Photograph with a Whole Mount Retinal Image

Clear fundus images could be obtained routinely under anesthesia, and mouse RGCs could be identified in vivo at the single-cell level.

By postural change, the superior, inferior, temporal, nasal, and central retina could be visualized. It was difficult, however, to take a photograph of the same living mouse and to achieve acceptable image quality in the peripheral retina, more than 1200 μm from optic disc, or even in the central retina in mice younger than 8 weeks or in those with corneal opacity.

Given that the mice were breathing during ocular fundus photography, a short exposure time was desirable to acquire clearer images without motion blur. However, short exposure time reduces the quality of the images, which was managed by combining three images. Because acute development of lens opacity is frequently encountered under general anesthesia in mice[17] and the pupil diameter of mice is smaller than that of rats, the image quality of mouse fundus photography had been limited. Covering the cornea with mineral oil not only keeps its surface smooth, it prevents the development of lens opacity. The excitation light was concentrated by a 40-D lens to pass small pupils.

To measure the resolution of ocular fundus photography, we compared the fundus photographs (Figs. 3A, 3B) and the images of the whole mount retina (Fig. 3C). This revealed that one pixel in a fundus photograph corresponded to a square of approximately 1.7 × 1.7 μm. The image of RGCs in the fundus photographs showed excellent concordance with that in the whole mount retina (Figs. 3B, 3C).

To verify that longitudinal recording of fundus photographs could be achieved with our methods, we took fundus photographs twice at intervals of 1 week and compared them. Even a single-cell loss could be visualized by our methods (Figs. 3D, 3E).

Reproducibility of Counting the Number of RGCs

To examine reproducibility, we took fundus photographs twice at intervals of 24 hours and counted RGCs manually in the same field of the four square fields, and then we calculated the intraclass correlation (ICC) and the coefficient of variation (CV) between the results obtained from the first and second photographs. The numbers of RGCs in the selected square field (220 × 220 pixels) were 187 ± 21 and 184 ± 22 (mean ± SD; $n = 10$) in the first and second photographs, respectively, the ICC was 0.941, and the CV was 2.1% ± 2.4% (mean ± SD). The density of RGCs in the four areas from nasal, superior, temporal, and inferior quadrants of the central retina were 1505 ± 89/mm^2, 1386 ± 111/mm^2, 1593 ± 139/mm^2, and 1563 ± 68/mm^2, respectively (Table 2). Among each of four areas, no statistical difference in the density of RGCs was seen (Kruskal-Wallis test; $P = 0.054$).

Longitudinal Evaluation of RGCs in Ischemia Reperfusion Models

We recorded fundus photographs longitudinally in the ischemia reperfusion model group and the sham-operated control group to evaluate the longitudinal changes in the number of RGCs in this experimental model. Figures 4A–4J indicate the longitudinal change in the RGC image in one eye after ischemia

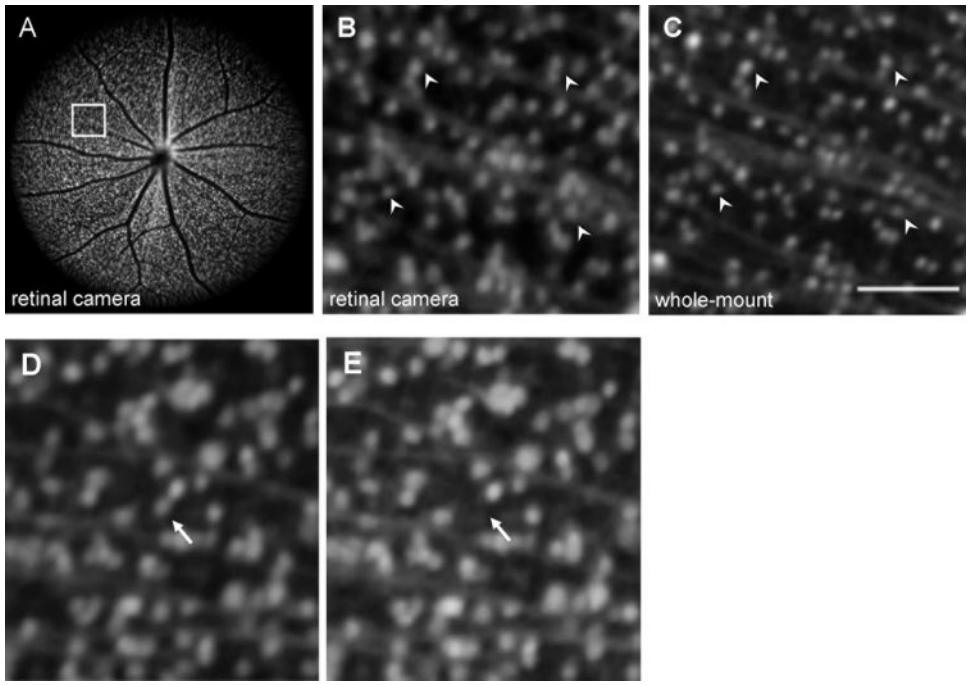

FIGURE 3. (**A**) Representative examples of mouse ocular fundus photographs. (**B**, **C**) Fundus photographs and whole mount of retina corresponding to the *insert* in (**A**). (**B**, **C**, *arrowheads*) Corresponding location. (**D**, **E**) RGC loss (*white arrow*) in the control eye could be detected clearly with our method. Scale bar, 100 μm.

TABLE 2. Density of CFP-Expressing RGCs (cells/mm^2) in the Four Areas of the Retina

	Mouse					
Area	**1**	**2**	**3**	**4**	**5**	**Mean ± SD**
Nasal	1525	1637	1511	1401	1449	1505 ± 89
Superior	1285	1381	1527	1271	1462	1386 ± 111
Inferior	1649	1402	1609	1527	1776	1593 ± 139
Temporal	1615	1583	1625	1461	1530	1563 ± 68

reperfusion injury, and Figures 4K and 4L indicate longitudinal change in that the control group.

Reduction of RGC numbers was evaluated sequentially in the same eyes. The number of RGCs and the fluorescence intensity of the nerve fiber decreased considerably during the first week. The percentages of RGCs decreased to 34.2% ± 7.5%, 24.1% ± 9.1%, 23.0% ± 9.3%, and 22.2% ± 8.4% (mean ± SD; $n = 5$) of the percentages before injury at 1, 2, 3, and 4 weeks after the injury, respectively ($P < 0.001$).

The percentages of RGCs in the control eyes were unchanged: 100.5% ± 4.1%, 100.4% ± 3.5%, 101.4% ± 2.3%, and 100.0% ± 3.0% (mean ± SD, $n = 7$) of the percentages before sham operation at 1, 2, 3, and 4 weeks, respectively. The percentages of RGCs with CFP fluorescence after injury to that before injury is shown in Figure 4M.

Histopathologic Evaluation

Figures 5A and 5B show a retinal section of a sham-operated control eye and of that of a treated eye 4 weeks after ischemia reperfusion injury, respectively.

The thickness of the RGC layer and the number of RGCs were markedly reduced in the ischemia reperfusion injury. Moreover, the thickness of the inner plexiform layer was reduced considerably in the ischemia reperfusion injury group

Figures 5C–5E indicate the retrogradely labeled RGCs with DiI in an eye of the ischemia reperfusion injury group in the whole mount retina 4 weeks after injury. In the ischemia reperfusion injury group, DiI$^+$ cells constituted 97.8% ± 3.1% (mean ± SD, five eyes of five mice) and DiI$^-$ cells constituted 2.2% ± 3.1% of the CFP$^+$ cells. Among the DiI$^+$ cells, CFP$^+$ cells constituted

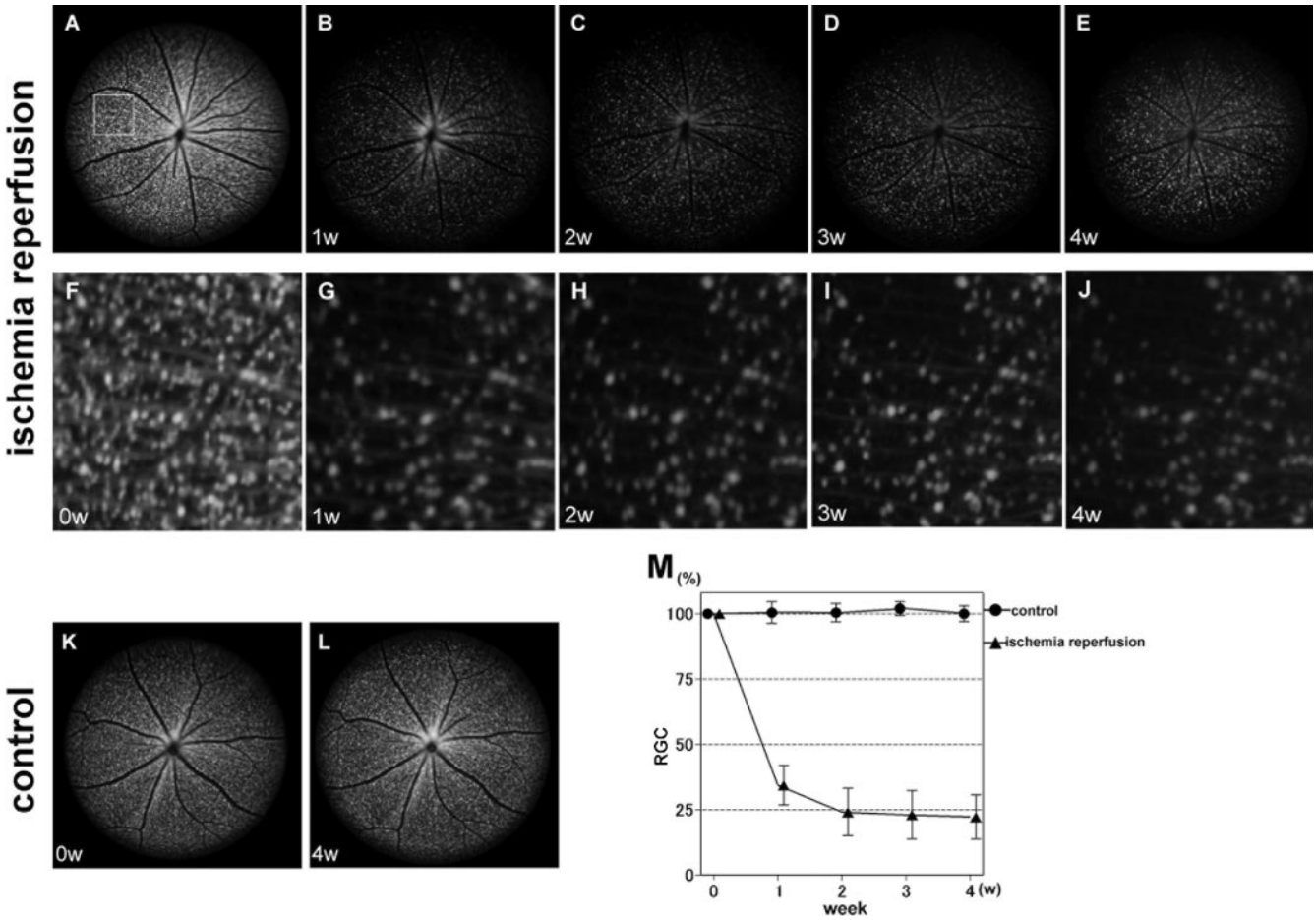

FIGURE 4. Longitudinal evaluation of the ischemia reperfusion injury model group. (**A**, **F**) Presurgery. (**B**, **G**) 1, (**C**, **H**) 2, (**D**, **I**) 3, and (**E**, **J**) 4 weeks after injury. (**F–J**) Corresponding area to the *insert* in (**A**). (**K, L**) Longitudinal evaluation of the control group. (**M**) Longitudinal changes of RGCs. The survival ratio of RGCs in postoperative period against that in the preoperative period in the control group ($n = 7$, *circles*) and the ischemia reperfusion injury model group ($n = 5$, *triangles*). Error bars indicate SD.

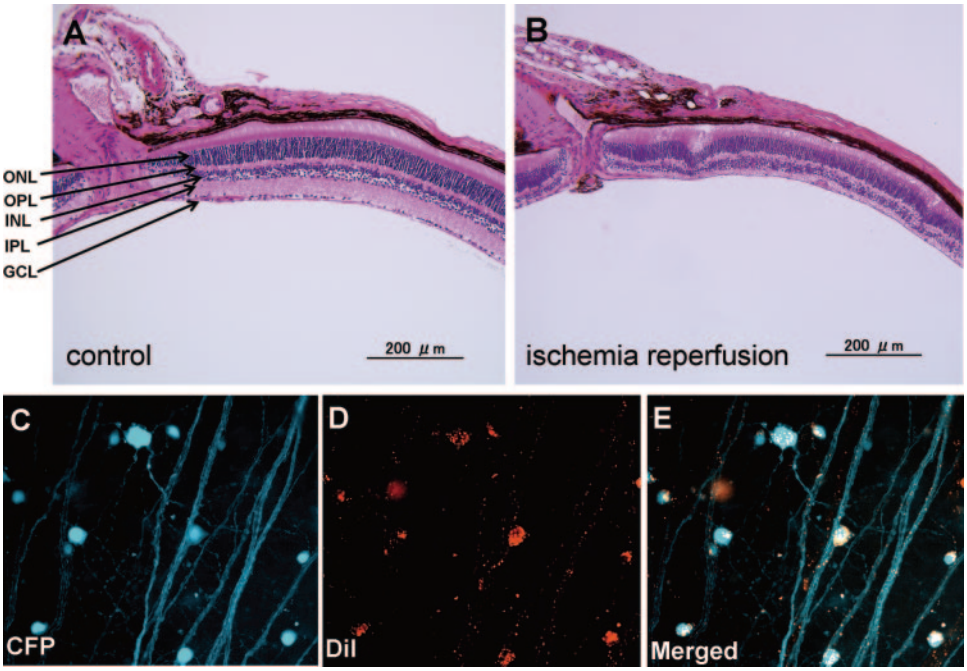

FIGURE 5. (**A**, **B**) Histologic evaluation of paraffin-embedded, hematoxylin/eosin-stained retinal sections. (**A**) Four weeks after sham operation and (**B**) 4 weeks after ischemia reperfusion injury. GCL, ganglion cell layer; IPL, inner plexiform layer; INL, inner nuclear layer; OPL, outer plexiform layer; ONL, outer nuclear layer. (**C–E**) Whole mount retina 4 weeks after ischemia reperfusion injury. Scale bars, 100 μm.

59.2% ± 3.4% and CFP^- cells constituted 40.8% ± 3.4% (Figs. 5C–E; Table 1). The percentage of the CFP^+ cells among the DiI^+ cells in the ischemia reperfusion injury group was significantly less than that in the control group ($P = 0.03$ by unpaired *t*-test; 59.2% ± 3.4% vs. 72.6% ± 5.2%).

DISCUSSION

Experimental mouse models are often applied to investigate the pathophysiology of human diseases. In vivo observation of apoptotic RGCs labeled with intravitreously injected Annexin V[18] and of retrogradely labeled RGCs after injection of a fluorescent dye into the superior colliculus[19] were reported in a rat model. Annexin V can bind to externalized phosphatidylserine, reflecting a preapoptotic condition,[18] but intravitreous injection may limit the experimental protocols and affect outcomes. Moreover, longitudinal counting of apoptotic RGCs was not performed in that study.[18] Fluorochromes such as DiA, DiI, and 4Di-10-ASP have often been used for labeling RGCs, but injection of exogenous dye into the superior colliculus is required, and sometimes RGCs are not labeled uniformly. Frequently used neurotracers are relatively stable, and microglia can be labeled secondarily by phagocytosing degenerated RGCs.[19,20] Lastly, genetic modification and experimental tools are less available in the rat than in the mouse.

Feng et al.[8] recently developed transgenic mice expressing CFP in living RGCs, which allowed us to visualize RGCs histologically. This mouse also paves the way for noninvasive observation of living RGCs in vivo. One of the benefits of the transgenic mouse is that it enables more precise cell counting than does the mouse with retrogradely labeled RGCs because CFP expression in the cytosol could delineate the cell body of RGCs whereas DiI is detected as particles in the RGC cytosol. Thus, some overlaid or adjacent cells were distinguished easily by the margin of CFP-stained cytosol (Figs. 2A–2C). Although our method relied on manual counting of CFP-stained RGCs as previous retrograde labeling method,[19] reproducibility of the result given by a masked, experienced investigator was thought to be sufficiently high.

In our devices, a pixel in the fundus photograph corresponds to approximately 1.7 × 1.7 μm, and an RGC soma measures 5 μm or more.[21] Thus, theoretically our system has sufficient resolution to detect an individual RGC. Comparison of ocular fundus images and the whole mount retina of the same eye confirmed that our method could capture almost all RGCs expressing CFP (Figs. 3B, 3C), and even the loss of a single cell could be detected with our method (Figs. 3D, 3E).

Available methods to evaluate experimental neurodegeneration by counting RGCs in the whole mount retina[22] or by measuring the thickness of retinal sections[12] require a large number of experimental animals and are limited in their ability to detect subtle changes in RGCs. We could detect RGC reduction with a smaller number of mice without sacrificing them by in vivo sequential imaging of the same region in a single eye.

Ocular fundus images of mice have been obtained in two ways: by means of a retinal camera[23] (a conventional method of fundus photography) and by cSLO.[14–16,24,25] In cSLO, the obtained image measures only 768 × 768 pixels,[26] and the detectable fluorescence is limited because of the limitation of available wavelength for excitation light (460 nm, 488 nm, 514 nm, 795 nm, and 830 nm).[14,25] Although these reports do not clearly mention the actual image area taken by one shot, montage photographs or several shots are required to evaluate a sufficiently wide area of the retina. On the other hand, approximately 25% of the whole RGCs (1700 × 1700 μm) can be longitudinally photographed in the same area of the same retina as one image by our method with a retinal camera. Moreover, a retinal camera, which is more cost-effective than cSLO, can support the use of various fluorescent dyes by changing fluorescence filters. One of the limitations is that RGCs in the peripheral retina 1200 μm or more apart from the disc could not be evaluated by our method because of the difficulty of taking images of acceptable quality. Thus, approximately central 36% of the whole area of the retina can be evaluated by the current method. This limitation that the whole retina could not be evaluated by our in vivo fundus photography also applied to the methods of in vivo imaging with Annexin V staining[18] or of scanning laser ophthalmoscopy.[19] In addition, it is challenging to take retinal photographs of mouse eyes younger than 8 weeks of age or with corneal opacity.

B6.Cg-Tg(Thy1-CFP)23Jrs/J mice express CFP in some amacrine cells, and all RGCs do not always express CFP.[8] Thus, with our method, some amacrine cells may be co-counted as a total number, but some RGCs may not be counted. However, CFP^+ and DiI^- cells, which are considered to be CFP^+ amacrine cells, were only 3% of the total CFP^+ cells, and CFP^+ and DiI^+ cells, which are considered to be CFP^+ RGCs, were approximately 73% of the total DiI^+ cells. Thus, any amacrine cells included should have only a minor effect on the RGC count.

One intriguing finding is that the percentage of CFP^+ cells among the DiI^+ cells in ischemia-reperfusion group 4 weeks after injury was significantly lower than that in the untreated group (59.2% vs. 72.6%). It was reported previously that $Thy1^+$ RGCs decrease rapidly after injury,[27,28] and Thy1 is a more sensitive marker of injured RGCs.[29] In our system, CFP^+ cells are thought to reflect $Thy1^+$ cells indirectly because the expression of CFP and Thy1 is linked genetically in this transgenic mouse. Thus, CFP^- RGCs after injury may reflect dysfunction of a basic cellular activity, gene transcription. On the other hand, DiI or other imported particles do not reflect cellular activity, even though they are observed in the cell body, because they can remain in the cells as long as the cell structure is conserved. In fact, our study indicated that injured RGCs after ischemia reperfusion detected by CFP fluorescent fadeaway progressed earlier than they did in other studies.[13] Thus, our system using CFP expression linked with Thy1 to detect cell injury may have advantages in the sensitivity to detect the earlier changes of cell death compared with other labeling methods.

In vivo imaging in neurodegenerative mouse models has many advantages.[30] By using our method to evaluate the number of RGCs longitudinally in the same animals, it is possible to monitor the time course of RGC injury or neuroprotective effects of drugs. Moreover, cross-breeding of various genetically modified mice and CFP-expressing mice would have great potential in investigating the time course of RGC death. Our technique may open up the possibility of detailed investigations of neurodegeneration or nerve regeneration through mouse eyes.

Acknowledgments

The authors thank Aya Iriyama and Masaaki Ohashi for histologic evaluation.

References

1. Burgoyne CF. Image analysis of optic nerve disease. *Eye.* 2004;18:1207–1213.
2. Fujimoto JG. Optical coherence tomography for ultrahigh resolution in vivo imaging. *Nat Biotechnol.* 2003;21:1361–1367.
3. Quigley HA. Number of people with glaucoma worldwide. *Br J Ophthalmol.* 1996;80:389–393.
4. Clark AF, Yorio T. Ophthalmic drug discovery. *Nat Rev Drug Discov.* 2003;2:448–459.
5. Goldberg I. Relationship between intraocular pressure and preservation of visual field in glaucoma. *Surv Ophthalmol.* 2003;48(suppl 1):S3–S7.
6. Fechtner RD, Weinreb RN. Mechanisms of optic nerve damage in primary open angle glaucoma. *Surv Ophthalmol.* 1994;39:23–42.
7. Goldblum D, Mittag T. Prospects for relevant glaucoma models with retinal ganglion cell damage in the rodent eye. *Vision Res.* 2002;42:471–478.
8. Feng G, Mellor RH, Bernstein M, et al. Imaging neuronal subsets in transgenic mice expressing multiple spectral variants of GFP. *Neuron.* 2000;28:41–51.
9. Shaner NC, Steinbach PA, Tsien RY. A guide to choosing fluorescent proteins. *Nat Methods.* 2005;2:905–909.
10. Harada C, Harada T, Slusher BS, Yoshida K, Matsuda H, Wada K. N-acetylated-alpha-linked-acidic dipeptidase inhibitor has a neuroprotective effect on mouse retinal ganglion cells after pressure-induced ischemia. *Neurosci Lett.* 2000;292:134–136.
11. Aihara M, Lindsey JD, Weinreb RN. Reduction of intraocular pressure in mouse eyes treated with latanoprost. *Invest Ophthalmol Vis Sci.* 2002;43:146–150.
12. Lam TT, Abler AS, Tso MO. Apoptosis and caspases after ischemia-reperfusion injury in rat retina. *Invest Ophthalmol Vis Sci.* 1999;40:967–975.
13. Lafuente MP, Villegas-Perez MP, Selles-Navarro I, et al. Retinal ganglion cell death after acute retinal ischemia is an ongoing process whose severity and duration depends on the duration of the insult. *Neuroscience.* 2002;109:157–168.
14. Seeliger MW, Beck SC, Pereyra-Munoz N, et al. In vivo confocal imaging of the retina in animal models using scanning laser ophthalmoscopy. *Vision Res.* 2005;45:3512–3519.
15. Luhmann UF, Lin J, Acar N, et al. Role of the Norrie disease pseudoglioma gene in sprouting angiogenesis during development of the retinal vasculature. *Invest Ophthalmol Vis Sci.* 2005;46:3372–3382.
16. Paques M, Simonutti M, Roux MJ, et al. High resolution fundus imaging by confocal scanning laser ophthalmoscopy in the mouse. *Vision Res.* 2006;46:1336–1345.
17. Calderone L, Grimes P, Shalev M. Acute reversible cataract induced by xylazine and by ketamine-xylazine anesthesia in rats and mice. *Exp Eye Res.* 1986;42:331–337.
18. Cordeiro MF, Guo L, Luong V, et al. Real-time imaging of single nerve cell apoptosis in retinal neurodegeneration. *Proc Natl Acad Sci U S A.* 2004;101:13352–13356.
19. Higashide T, Kawaguchi I, Ohkubo S, Takeda H, Sugiyama K. In vivo imaging and counting of rat retinal ganglion cells using a scanning laser ophthalmoscope. *Invest Ophthalmol Vis Sci.* 2006;47:2943–2950.
20. Thanos S, Kacza J, Seeger J, Mey J. Old dyes for new scopes: the phagocytosis-dependent long-term fluorescence labelling of microglial cells in vivo. *Trends Neurosci.* 1994;17:177–182.
21. Perry VH. Evidence for an amacrine cell system in the ganglion cell layer of the rat retina. *Neuroscience.* 1981;6:931–944.
22. Inoue T, Hosokawa M, Morigiwa K, Ohashi Y, Fukuda Y. Bcl-2 overexpression does not enhance in vivo axonal regeneration of retinal ganglion cells after peripheral nerve transplantation in adult mice. *J Neurosci.* 2002;22:4468–4477.
23. Hawes NL, Smith RS, Chang B, Davisson M, Heckenlively JR, John SW. Mouse fundus photography and angiography: a catalogue of normal and mutant phenotypes. *Mol Vis.* 1999;5:22.
24. Jaissle GB, May CA, Reinhard J, et al. Evaluation of the rhodopsin knockout mouse as a model of pure cone function. *Invest Ophthalmol Vis Sci.* 2001;42:506–513.
25. Leung CK, Lindsey JD, Crowston JG, et al. In vivo imaging of murine retinal ganglion cells. *J Neurosci Methods.* 2008;168:475–478.
26. Jorzik JJ, Bindewald A, Dithmar S, Holz FG. Digital simultaneous fluorescein and indocyanine green angiography, autofluorescence, and red-free imaging with a solid-state laser-based confocal scanning laser ophthalmoscope. *Retina.* 2005;25:405–416.
27. Schlamp CL, Johnson EC, Li Y, Morrison JC, Nickells RW. Changes in Thy1 gene expression associated with damaged retinal ganglion cells. *Mol Vis.* 2001;7:192–201.
28. Huang W, Fileta J, Guo Y, Grosskreutz CL. Downregulation of Thy1 in retinal ganglion cells in experimental glaucoma. *Curr Eye Res.* 2006;31:265–271.
29. Chidlow G, Casson R, Sobrado-Calvo P, Vidal-Sanz M, Osborne NN. Measurement of retinal injury in the rat after optic nerve transection: an RT-PCR study. *Mol Vis.* 2005;11:387–396.
30. Misgeld T, Kerschensteiner M. In vivo imaging of the diseased nervous system. *Nat Rev Neurosci.* 2006;7:449–463.